Original Research *Feature article*

miR-31 promotes neural stem cell proliferation and restores motor function after spinal cord injury

Xiao Li[1], Yuantao Gao[2], Feng Tian[1], Ruochen Du[1], Yitong Yuan[1], Pengfei Li[1], Fang Liu[1] and Chunfang Wang[1]

[1]Laboratory Animal Research Center of Shanxi Medical University, Shanxi Key Laboratory of Animal and Animal Model of Human Diseases, Taiyuan 030001, China; [2]Queen Mary School, Nanchang University, Nanchang 330000, China
Corresponding author: Chunfang Wang. Email: Wangchunfang@sxmu.edu.cn

Impact statement

miR-31 has embryonic specificity in regulating cell proliferation, and its expression is higher in neural stem cells (NSCs) than in motor neurons. miR-31 induced the proliferation of NSCs by upregulating the Notch signaling pathway, while Notch was inhibited by miR-31 inactivation. Injection of miR-31 agomir into mouse models of spinal cord injury (SCI) could effectively restore motor functions after SCI. The results suggest that miR-31 might play a crucial role in nervous system development. The results could suggest new methods for SCI treatment. Indeed, miR-31 agomir injection at the initial stage of injury could promote NSC proliferation and enhance the recovery effect. Future studies will have to look at the interaction between miR-31 and other factors known to influence SCI repairs, such as IL-34 and vitamin D.

Abstract

This study aims to examine whether miR-31 promotes endogenous NSC proliferation and be used for spinal cord injury management. In the present study, the morpholino knockdown of miR-31 induced abnormal neuronal apoptosis in zebrafish, resulting in impaired development of the tail. miR-31 agomir transfection in NSCs increased Nestin expression and decreased ChAT and GFAP expression levels. miR-31 induced the proliferation of mouse NSCs by upregulating the Notch signaling pathway, and more NSCs entered G1; Notch was inhibited by miR-31 inactivation. Injection of a miR-31 agomir into mouse models of spinal cord injury could effectively restore motor functions after spinal cord injury, which was achieved by promoting the proliferation of endogenous NSCs. After the injection of a miR-31 agomir in spinal cord injury mice, the expression of Nestin and GFAP increased, while GFAP expression decreased. In conclusion, the zebrafish experiments prove that a lack of miR-31 will block nervous system development. In spinal cord injury mouse models, miR-31 overexpression might promote spinal cord injury repair.

Keywords: Spinal cord injury, miR-31, zebrafish, neural stem cells, NOTCH, cell proliferation

Experimental Biology and Medicine **2021; 246: 1274–1286. DOI: 10.1177/1535370221997071**

Introduction

Motor function restoration remains an issue in spinal cord injury (SCI) management. Studies suggested that the injection of neural stem cells (NSCs) can effectively treat SCI, but the supplies of NSCs are restricted by ethical and practical issues. Some researchers are aiming at determining new methods to obtain cells that could be used for SCI treatment. For example, Salewski *et al.* developed a method to induce NSCs from embryonic stem cells.[1] Although this approach can solve the problem of NSC supply, the treatment risks such as immune rejection must be considered. There are some undifferentiated NSCs in the spinal cord, which will proliferate naturally after SCI and participate in repair after injury.[2] Therefore, it can be hypothesized that stimulating the proliferation of those NSCs could achieve some therapeutic effect. microRNAs (miRNAs) are non-coding small RNAs that regulated mRNAs negatively by binding to them and favoring their degradation and are involved in the regulation of cellular processes, including differentiation and cell proliferation. In order to understand the changes in miRNA over the process of NSC differentiation, a previous study by our group examined the differential expression of the miRNAs of NSCs and motor neurons and found that miR-31 was expressed at high levels in NSCs and lowly expressed in motor neurons.[3] As an embryo-specific miRNA,[4] miR-31 levels are significantly higher on the seventh day after SCI compared with before injury.[5–7] miR-31 can promote the proliferation of a variety of cell types.[8–10] Still, the exact involvement of miR-31 in NSC proliferation remains unknown.

In order to study the effect of miR-31 on NSCs, we created a miR-31 morpholino (MO) knockout model in EGFP-HB9+ transgenic zebrafish to observe the effect of miR-31 knockout on neurons. Mouse NSCs were used to examine the changes in relevant signaling pathways. This study also examined the effect of miR-31 agomir and antagomir to explore the therapeutic effect of miR-31 on SCI mouse models. The data could suggest new methods for SCI treatment.

Materials and methods

Animals

Adult wild-type AB zebrafish (Shanghai Research Center for Model Organisms) were maintained in 28.5°C water and exposed to a 14/10-h light/dark cycle. A total of five to six parental pairs of zebrafish were mated naturally, and 200–300 embryos were obtained by parental pairs. The embryos were kept in the same water type (deionized water with 0.2% instant ocean salt). The stages of the embryos were determined according to a previous study.[11] NSCs were identified using Nestin staining. The hb9-EGFP transgenic lines were established as previously described.[12] The zebrafish facility of the Shanghai Research Center for Model Organisms is accredited by the International Association for Assessment and Accreditation of Laboratory Animal Care.

Adult ICR mice (eight weeks, 18–20 g, Laboratory Animal Center of Shanxi Medical University) were kept at 26°C and 40%–60% humidity and exposed to a 14/10-h light/dark cycle. All means were taken to minimize animal suffering and lower the number of animals used. The animal study protocol was approved by the Ethics Committee of Shanxi Medical University. The 12–14 days pregnant mice were anesthetized with pentobarbital, and the NSCs were isolated by a routine method.[13] The medium for NSCs was NeuroCult™ Proliferation Kit (#05702, STEMCELL Technologies Inc., Canada). The SCI mouse model was produced using an IMPACTOR III device (New York University, New York, USA).[14] The impact height for mice was 6.25 cm. The inability of the hind limbs of the mouse to move on the first day after modeling was considered as successful modeling.

Microinjections in zebrafish

The MO was designed by Gene Tools, LLC (http://www.gene-tools.com/). The fertilized one-cell stage embryos were microinjected with antisense MO (GeneTools, LLC, Philomath, OR, USA).[15] The miR-31 sequence MO was 5′-TTA ACA GCT ATG CCA ACA TCT TGC C-3′,[16] and the standard control MO sequence was 5′-CCT CTT ACC TCA GTT ACA ATT TAT A-3′. For the miR-31 knockdown study, control MO or miR-31 MO (8 ng) was injected. Then, the embryos were rinsed in fish water and incubated. To ease the observation, the embryos were anesthetized with 0.016% tricaine (Sigma-Aldrich, St Louis, MO, USA) in fish water.

Zebrafish behavioral assay

The 48-h-old zebrafish were pooled together and dechorionated by hand at least 3 h before the experiment. The escape response was evaluated by touching the fish with a fine needle at least two times, either at the dorsal tip of the tail or on the trunk. A reduced escape response was defined as a movement of less than three fish lengths. A camera was used to capture one experiment.

Acridine orange staining

Embryos injected with control or miR-31 MO were placed in 5 μg/mL AO in fish water (Sigma-Aldrich, St Louis, MO, USA) for 60 min at 26 and 48 h post-fertilization (hpf). They were then washed with fish water three times, 5 min each time, and anesthetized with 0.016% tricaine (Sigma-Aldrich, St Louis, MO, USA), followed by an orientation on the lateral side. Subsequently, the fishes were mounted with methylcellulose for fluorescence microscopy (SMZ-1500, Nikon, Tokyo, Japan). The quantitative image analysis was carried out using an image-based morphometric analysis method (NIS-Elements D3.1, Nikon, Tokyo, Japan). Adobe Photoshop 7.0 (Adobe, San Jose, CA, USA) was used to adjust the images (levels, brightness, contrast, hue, and saturation) to optimize the visualization of the patterns of expression. A total of 10 animals were quantified for each treatment, and the overall signal per animal was averaged.

Zebrafish spinal motor neuron evaluation

To evaluate the spinal motor neurons formation, 8 ng of control or miR-31 MO was injected in the fertilized one-cell hb9-EGFP transgenic zebrafish. The fishes were dechorionated at 48 hpf, anesthetized with 0.016% MS-222, oriented on the lateral side (anterior, left; posterior, right; dorsal, top), and mounted with 3% methylcellulose for fluorescence microscopy (SMZ-1500, Nikon, Tokyo, Japan) to analyze the phenotypes of the spinal motor neurons. The images were analyzed as above.

Mouse motor function scoring

The motor function recovery of both lower limbs was observed in an open area at the same time every day for one to eight weeks after spinal cord injury. Posterior limb recovery was assessed by the BMS score.[17] The hind legs of the mice were coated with ink, and they were allowed to climb over a screen paper. The number of errors on the soles of their hind legs was calculated over 20 steps. The evaluation was carried out in a double-blind manner and independently by two well-trained individuals. The left and right hind limbs were evaluated.

Agomir and antagomir treatment

The *in vitro* analyses were divided into the miR-31 agomir, miR-31 antagomir (Ruibo Ltd, Guangzhou, China), and control groups. Cells were inoculated in a six-well plate at 2×10^5 cells/mL and 30 pmol of nucleotides were transfected (Ruibo Ltd, Guangzhou, China), according to the

instructions from the manufacturer. In SCI mouse models, miR-31 agomir, miR-31 antagomir, or saline were injected using a microsyringe pump at four points around the injury site at 20 nmol/mL. In order to avoid secondary spinal cord damage caused by the repeated opening of the laminae, we injected the mouse spinal cord injury site with agomir/antagomir/saline after SCI was successfully modeled, i.e. without bleeding and with stable breathing. The animals were treated for three days.

Real-time PCR

The miRNAs were extracted using a commercial kit (mirVana^{TM} miRNA Isolation Kit, Ambion, Thermo Fisher Scientific, Waltham, MA, USA). The miRNAs were reverse-transcribed into cDNA using the TaqMan^{TM} MicroRNA Reverse Transcription using U6 (RT001973) and miR-31 (RT000185). Subsequently, U6 (TM001973) was the internal reference, and the changes in the expression of miR-31 (TM000185) were detected by real-time PCR. Total RNA was extracted using Trizol at one and three days after treatment and reverse-transcribed into cDNA (PrimeScript RT Master Mix, TAKARA). Fluorescence quantitative PCR (ABI 7300, Applied Biosystems, Foster City, CA, USA) was used to detect the changes in mRNA expression of ChAT, Nestin, and GFAP. Rpl-19 was the internal reference. Table 1 lists the primers used for PCR.

Immunofluorescence

Cells (2×10^5) were plated in a six-well plate containing coverslips. At one and three days after treatment, the cells were fixed, titrated, and blocked using goat serum. Primary antibodies against Nestin, ChAT, and GFAP (all from Abcam, Cambridge, United Kingdom) were incubated at 4°C overnight. The CY3-labeled secondary antibody (Abcam, Cambridge, United Kingdom) was added and incubated for 2 h at room temperature. Hoechst was used for counterstaining. A fluorescence microscope (BX51, Olympus, Tokyo, Japan) was used to observe and count the cells.

Western blot

Total proteins from transfected cells and spinal cords were extracted from protein lysate and 1% PMSF. The BCA assay was used to determine the protein concentraions. Proteins (30 μg) were resolved by 10% SDS-PAGE and blotted to PVDF membranes, which were blocked using 5% skim milk. They were incubated with the primary antibody against Nestin, ChAT, GFAP, or GAPDH (all from Abcam, Cambridge, United Kingdom). The corresponding horseradish peroxidase-conjugated secondary antibodies were added and revealed by electrochemiluminescence. The blots were scanned and analyzed using Image J (National Institutes of Health, Bethesda, MD, USA).

Table 1. Primers used for real-time PCR.

Gene	Forward primer (5′–>3′)	Reverse primer (5′–>3′)
Zebrafish RT-PCR primers		
Numb	CGATGGGCTGAGGGTTGT	CCTTCTCTATCGTCTGGTCAAGGAT
Notch1A	TCTTGGTGAAATTAACGCTACTGACT	TGGGCTTGTACTCGCATATTCC
Wnt1B	GAGGCTGCAGCGACAATGT	CTCGCTGGAATCCACAAACTC
AXIN-1	CCCTCTCTGGCCAATCACA	AGAGTAGCGACCACCATAATGCT
Ctnnb	CGCTGCGGGTTGTTCTCT	TCAGCACGTAAAACGCGAAT
Nestin	CCAGGGATGGGCAAACTTG	CAGGTGTGTTTGATTAGTGTTGGAA
Neurod	GACGGGCACTCGCATCA	AGTCGTGAAATATCGCGTTCAA
HB9-1	CCGACGCACTCCAGACAGA	GGGAATCAAGCCGCAAGA
HB9-2	GAAACCAGGGCTGCTCAATC	GTCGTGTACATGCCTGGGATAG
GFAP	CAGAAAATAACCTCAACACCTTCAGA	GCTGCACGCGGTTCAGA
HDR	ATGGCATTGGGACGCAATCT	AGCCTTCCCTGCATGAAACA
Cas-a	CAGAAAACGACTGGCCTTGC	GAGCAAAGTCCCTGATGGCT
Cas-3a	AGCCTCAATCCCATGCCTTC	TGCGCAACTGTCTGGTCATT
Cas-8	GACCAGGAACAAGGAGGCAG	GCCGCTGGGTCAGTATGTAAT
ef1α	GGAAATTCGAGACCAGCAAATAC	GATACCAGCCTCAAACTCACC
Mouse RT-PCR primers		
ChAT	CAGAAGGCTGAGGTGGAAATG	CTGCTGAGGAGGCGAGATG
Nestin	GGTCACTGTCGCCGCTACTC	AAGCGGACGTGGAGCACTA
GFAP	AGAAGCCGATGTAGGACCGTATAG	TCCCCTTGAGCCCCTAAAA
NOTCH	TCGTGTGTCAAGCTGATGAGGA	GTTCGGCAGCTACAGGTCACAA
Math1	ACATCTCCCAGATCCCACAG	GGGCATTTGGTTGTCTCAGT
Neurog	CATTTGCAATGGCTGGCATC	CAATAGGCATTGTGACGAATCTGG
HB9	CGAGACTCAGGTGAAGATTTGGT	CTGCTCTTTGGCCTTTTTGC
PS1	AGTCAAGAGCTGCTGTCCAGGAA	GCTGAGGCCTTACCAACCAGAA
Mash1	AAGAGCTGCTGGACTTTACCAACTG	ATTTGACGTCGTTGGCGAGA
Hes1	GCAGACATTCTGGAAATGACTGTGA	GAGTGCGCACCTCGGTGTTA
Numb	TCCCAGATCACCAGTGCCTTC	CTAACCAGCGGTCAGCTTCAGAG
RBPJ	ACAAACTGTGCACCTGCGTGTAA	ATCGGGCACATCCCACAGA
SOX1	GCCCTCGGATCTCTGGTCAA	CTGATCATCTCGCGCAGGTC

Flow cytometry

The NSCs were centrifuged to remove the supernatant. The cells were resuspended with Accumax (2 mL), incubated at 37°C for 10 min, and 5 mL of DPBS was added and mixed. The cells were seeded on a 6-well plate for overnight culture. BrdU was added to 10 g/mL. The cells were incubated for 20 min, washed with PBS twice, fixed in 70% ethanol overnight at −20°C, denatured for 45 min in 2 N HCL, incubated with a FITC-labeled secondary antibody at room temperature for 1 h, and finally incubated with 200 g/mL PI for 30 min and 40 g/mL RNase A. Flow cytometry was used to detect cell cycle changes.

Statistical analysis

All zebrafish data are described as means ± standard error. The statistical analyses and graph creation were performed using GraphPad Prism 5.0 (GraphPad Software, San Diego, CA, USA). The data were analyzed using the Student's *t*-test or the Chi-square test. All mouse data were analyzed using SPSS 17.0 (IBM, Armonk, NY, USA). One-way analysis of variance (ANOVA) followed by unpaired Student's *t-test* was carried out to compare the groups in the BMS test and grid test. $P < 0.05$ was considered statistically significant.

Results

miR-31 knockdown induces abnormal motor neuron outgrowth in zebrafish

Compared with the control group, 48-hpf miR-31 knockout led to a lack of neurons in the zebrafish, especially motor neurons (Figure 1(a) to (h) and Supplementary Figure S1). The notochord was small. In the control group, the notochord was fine, and the fluorescence intensity was high (Figure 1(b) to (d)). After miR-31 MO knockout, the zebrafish escape reaction disappeared. Control zebrafish could escape distances of >3 times their length. miR-31 MO zebrafish did not show free swimming. The control group

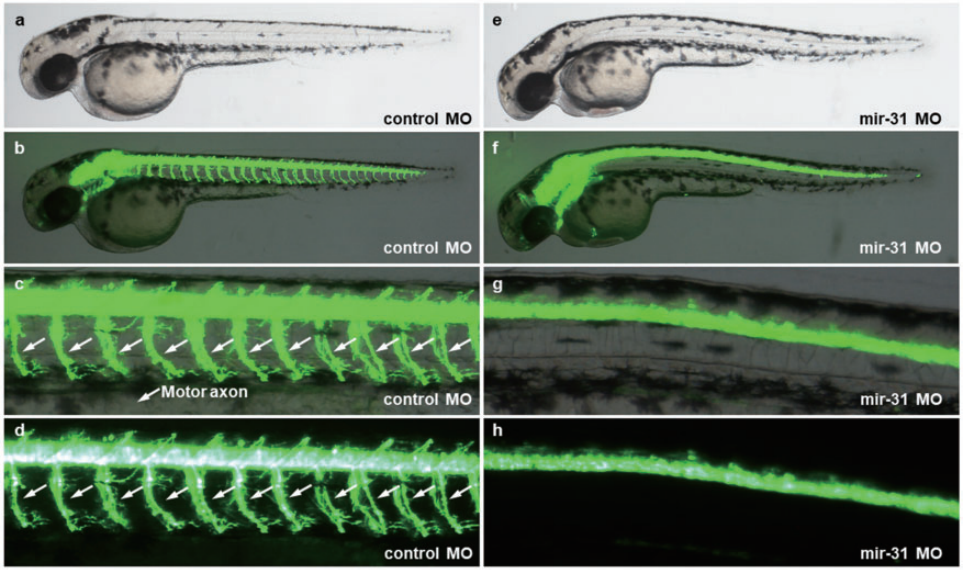

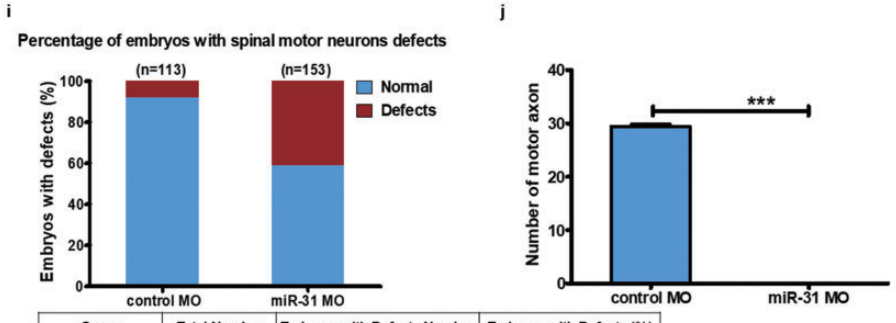

Group	Total Number	Embryos with Defects Number	Embryos with Defects (%)
8ng control MO	113	9	7.96
8ng dre-miR-31 MO	153	62	40.52

Figure 1. miR-31 knockdown induces abnormal motor neuron outgrowth. Tg (hb9:EGFP) zebrafish embryos were injected with 8 ng of control or miR-31 MO. (a–h) Representative bright field and fluorescent images of Tg(hb9:EGFP) embryos at 48 hpf. (b–d) Image of trunk regions taken at 48 hpf, with the spinal motor neurons structures visualized by eGFP fluorescence and labeled motor axon (white arrows), showed normal development in the embryo injected with the control MO. Compared with the control MO, embryos injected with miR-31 MO present a lower number of incomplete motor axons (f–h). The percentage of embryos with spinal motor neurons defects (i). The bar graph shows the percentage of embryos with motor axon defects. The stereotypic escape response was abnormal in miR-31 morphants at 48 hpf. (j) Quantification of the number of complete motor axons shows a significant decrease in miR-31 MO-injected embryos. Columns, mean; bars, SEM ($n = 10$; unpaired student's *t*-test), ***$P < 0.0001$. hpf: hours post-fertilization. (A color version of this figure is available in the online journal.)

showed an embryonic defect rate of 8.0%, compared with 40.5% in the miR-31 MO group. Besides, there were no motor neurons in the miR-31 MO group (Figure 1(j)). Hence, miR-31 knockout seriously affects the neuronal development of zebrafish, with significant loss of motor function.

Morpholino knockdown of miR-31 induces potent CNS-specific apoptosis

AO was used in 26-hpf zebrafish to observe apoptosis. The apoptotic cells were rare in the control group, while the central nervous system (CNS) in the miR-31 MO group showed a large number of apoptotic cells along the notochord (Figure 2(a) to (h) and Supplementary Figure S2). In the miR-31 MO group, there was an average of 125.9 apoptotic bodies per zebrafish, compared with five in controls (Figure 2(m)). Therefore, the knockout of miR-31 leads to significant apoptosis in the CNS.

In order to observe zebrafish tissue apoptosis, we used the same method to examine 48-hpf zebrafish. In the control group, only a small amount of apoptotic cells was found, and not specifically in the spinal cord (Figure 3(a) to (d) and Supplementary Figure S3). The miR-31 MO group showed apoptotic cells along the notochord, but with a different distribution compared with 26-hpf zebrafish. In the axon area, there was only a small amount of apoptotic cells, and the tail had a large number of apoptotic cells (Figure 3(e) to (h) and Supplementary Figure S3). Through quantitative analysis, the miR-31 MO group showed 122 times higher apoptotic cells than the control group (Figure 3(i)). Supplementary Figure S3 shows that the 26-hpf zebrafish had abnormal development compared with the control ones, with large numbers of apoptotic cells scattered in the abnormally developed body parts. These data suggest that apoptosis does not weaken with development. Furthermore, Supplementary Figure S4 shows that the miR-31-knockdown zebrafishes had abnormal development compared with the control ones, with abnormal heart development and pericardial edema.

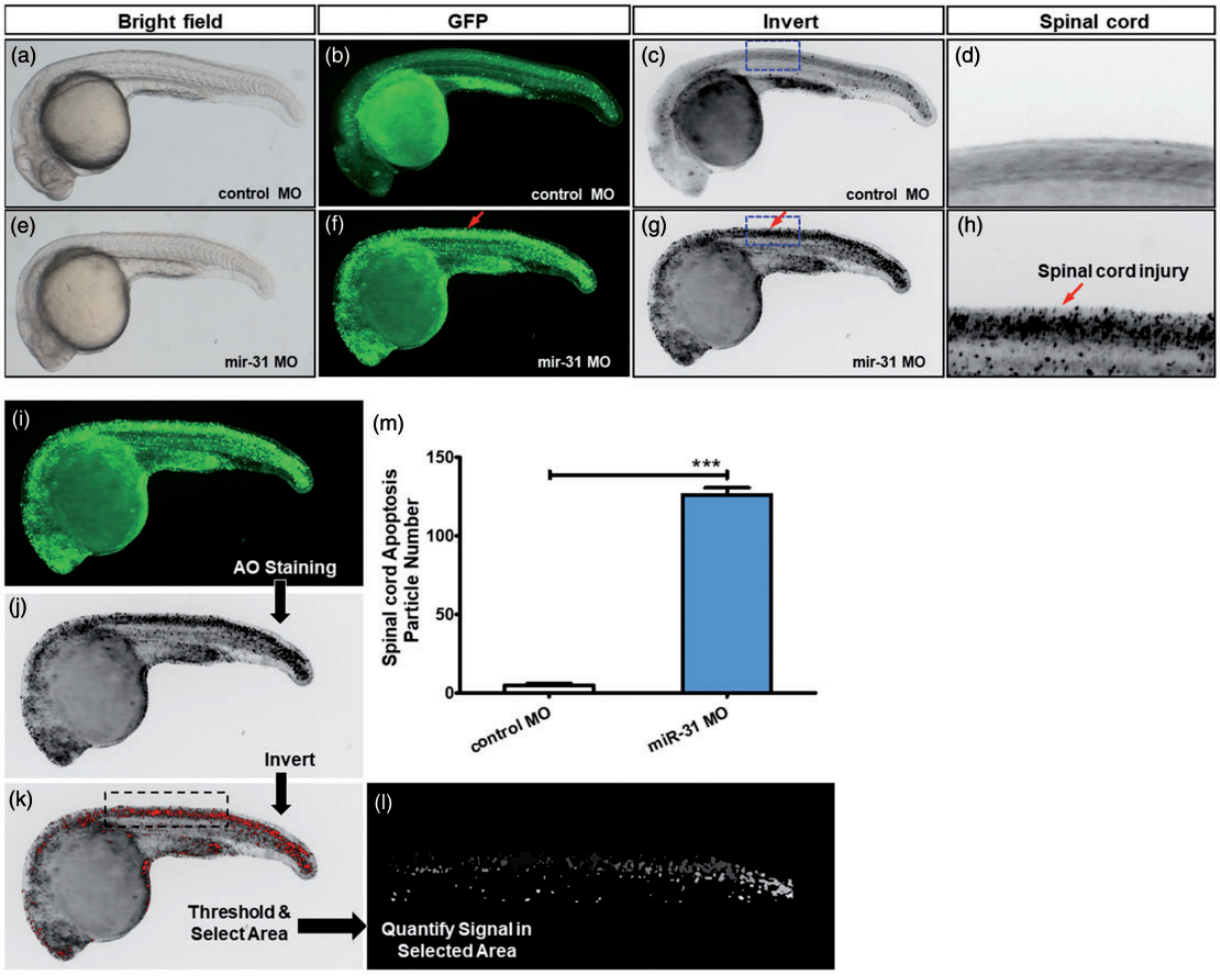

Figure 2. miR-31 knockdown induces CNS-specific apoptosis. Embryos injected with control or miR-31 MO were stained with acridine orange (AO) at 26 hpf. The apoptotic cells are shown as bright green spots or black spots. Less bright homogenous green or black is unspecific background staining. (a–d) Controls exhibited few or no apoptotic cells in the central nervous system (CNS). In contrast, significantly increased staining was observed throughout the CNS in zebrafish injected with miR-31 MO (f–h, red arrows). The blue box area is shown with higher magnification in the right panels. (i–m) Quantification of apoptosis number in the spinal cord shows a 25-fold increase in miR-31 morphants ($n = 10$) at 26 hpf. A-H: lateral view, anterior, left; hpf: hours post-fertilization. Columns, mean; bars, SEM. (A color version of this figure is available in the online journal.)

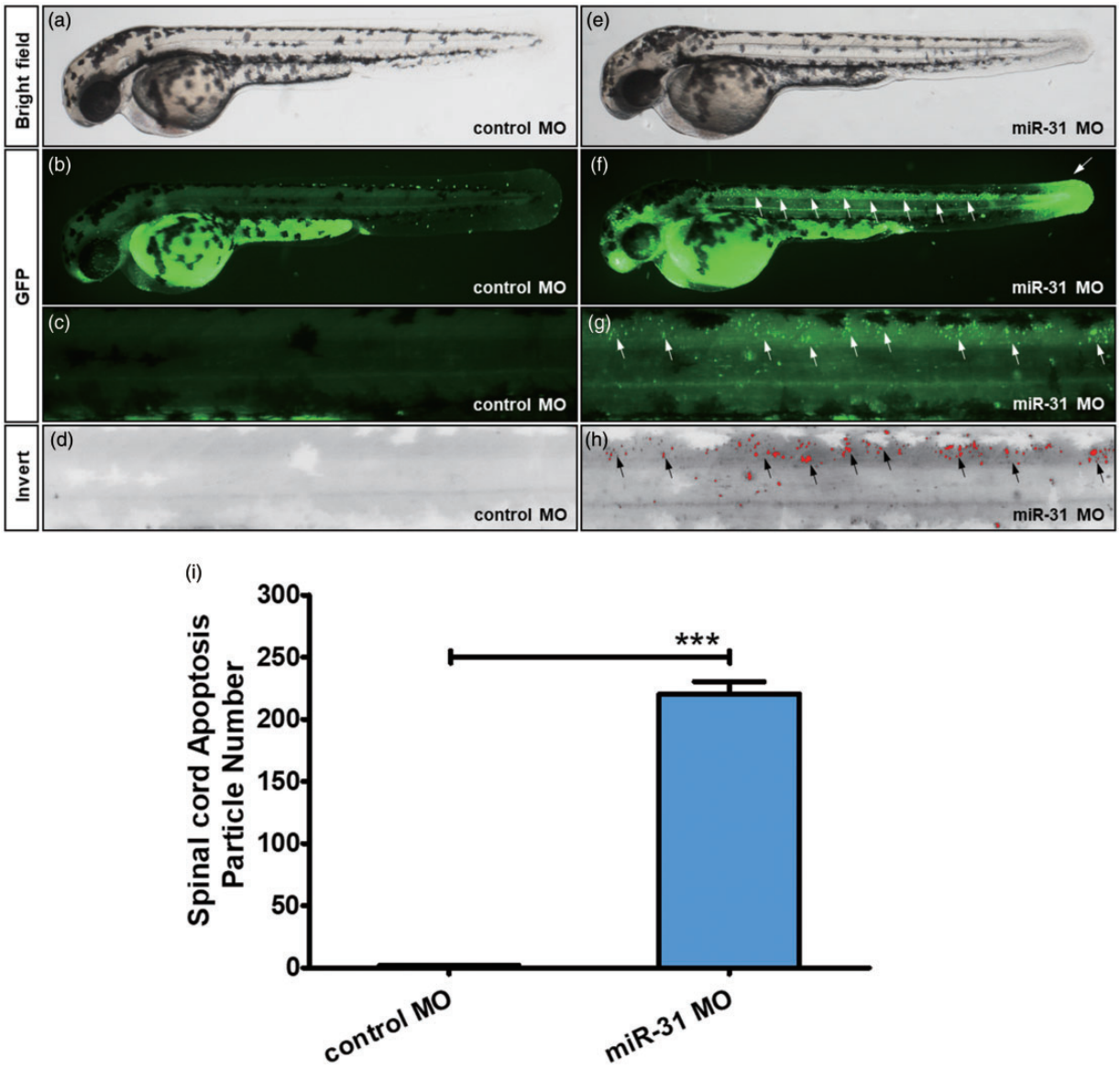

Figure 3. Morpholino knockdown of miR-31 induces apoptosis in the CNS and tail. Embryos injected with control (a–d) or miR-31 MO (e–h) were stained with acridine orange (AO) at 48 hpf. Apoptotic cells are shown as bright green spots or red spots, and less bright homogenous green or black is unspecific background staining. (b–d) Control MO zebrafish exhibited few or no apoptotic cells in the whole body. In contrast, high staining was observed throughout the CNS and tail in zebrafish injected with 8 ng of miR-31 MO (f–h, white arrows, and black arrows). (i–n) Quantification of apoptotic bodies at the spinal cord shows a 122-fold increase in miR-31 morphants ($n = 10$) at 48 hpf. A-M: lateral view, anterior, left; hpf: hours post-fertilization. Columns, mean; bars, SEM. (A color version of this figure is available in the online journal.)

miR-31 is transfected to neural stem cells

Nestin was detected in isolated NSCs (Figure 4(a)). As the miRNAs were conjugated with Cy3, fluorescence intensity reflected the presence of transfected miR-31. As expected, miR-31 expression was significantly higher than in the other groups (Figure 4(b)). Further analysis revealed that miR-31 and Nestin co-localized in cells (Figure 4(c)). These findings indicate that the modified miR-31 was successfully transfected into NSCs.

Effect of miR-31 on neural stem cells after transfection

One day after transfection, the expression of Nestin was elevated in the agomir group and lower in the antagomir group. Nestin expression in the agomir and antagomir groups was both decreased after three days, but the expression in the agomir group was still higher than in the antagomir group. ChAT expression was higher in the agomir group and lower in the antagomir group at one day. The expression of ChAT in the antagomir group was higher than in the agomir group at three days. The agomir group showed a higher expression of GFAP than the antagomir group, regardless of time (Figure 5(a)). The protein expression of Nestin was higher in the agomir group and lower in the antagomir group. The expression of ChAT was the highest in the antagomir group, and there were no differences in the expression of ChAT between the agomir and control groups. Compared with the other groups, the expression of GFAP was lower in the agomir group (Figure 5(b)).

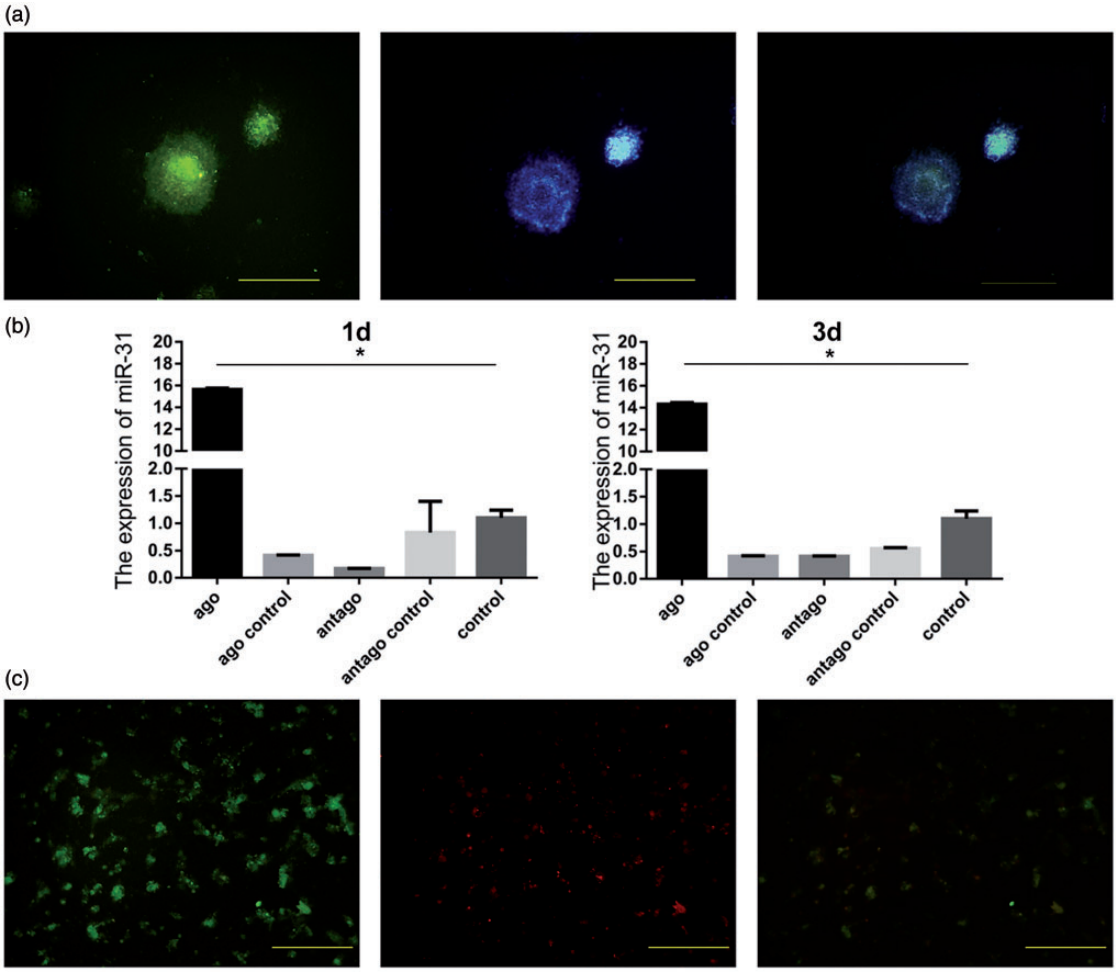

Figure 4. Identification of neural stem cells cultured *in vitro* and detection of miR-31 after transfection. Green cells are positive for Nestin; blue indicates cell nuclei stained with Hoechst. They are overlapping after merging (a). miR-31 was overexpressed in the agomir group and lowly expressed in the antagomir group (b). Positive cells for miR-31 are red, and they overlap with Nestin-positive cells (c). Scale bar = 10 μm. $^*P < 0.05$. Columns, mean; bars, SEM. (A color version of this figure is available in the online journal.)

Immunofluorescence showed that the agomir group had the highest proportion of Nestin-positive cells at one day, while the antagomir group had the lowest Nestin-positive cell numbers at three days. ChAT expression showed the opposite trend. The antagomir group had the highest proportion of ChAt-positive cells at three days, while the agomir group had the lowest ChAt expression (Figure 5 (c)). Flow cytometry showed that in the agomir group, the cells in the S phase were 42.4%, compared with 37.2% for the antagomir group and 35.2% for controls, showing that miR-31 overexpression increased cell proliferation and vice versa (Figure 6).

miR-31 injection can promote recovery of SCI mice

The motor function score was used to evaluate the effects of miRNAs treatment in mice with SCI. As expected, the motor function gradually recovered in all groups, but compared with the other groups, the score in the miR-31 group was higher from four weeks and thereafter (Figure 7(a)), while the foot misplacement rate in the miR-31 group was lower (Figure 7(b)).

Molecular analysis of mir-31 in SCI mice after injection

miR-31 expression was improved after miR-31 agomir injection in mice. miR-31 could not be detected in the antagomir group. The expression of Nestin was similar between the agomir and control groups, and it was lower in the antagomir group. Hence, miR-31 might help maintain the stemness of NSCs. ChAT expression was the highest in the agomir group. The expression of GFAP was the same (Figure 8(a)).

The protein expression of Nestin was found to be the highest in the agomir group, while the antagomir group showed the lowest. Among all groups, the expression of ChAT was higher in the antagomir group and lower in the agomir group, and the expression of GFAP was higher in the agomir group and lower in controls (Figure 8(b)).

Discussion

The present study strongly suggests that MO knockdown of miR-31 induced abnormal motor neuronal outgrowth and induced neuronal apoptosis in zebrafish (Figure 1). At 48 hpf, many apoptotic cells were found in the brain,

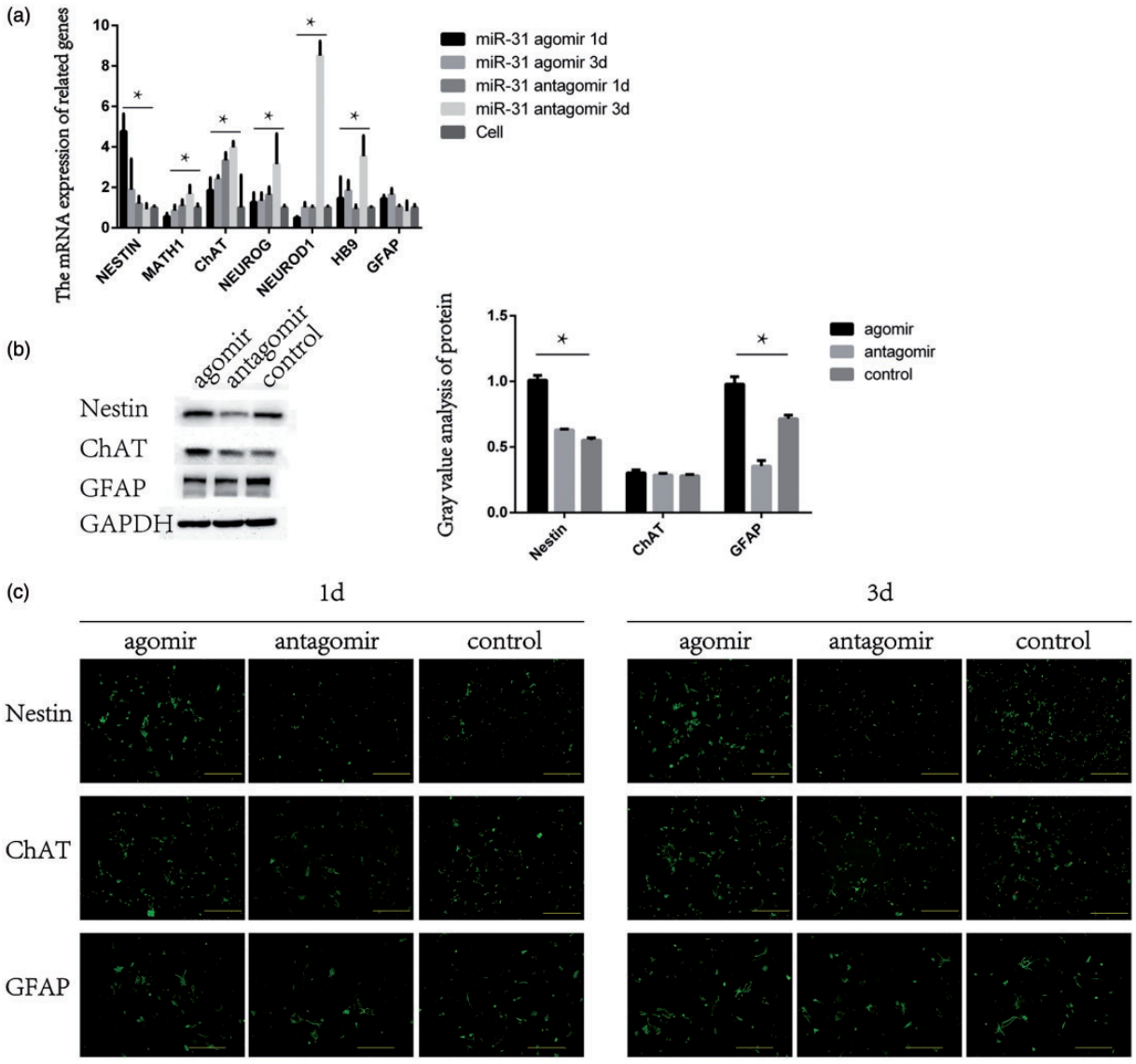

Figure 5. The mRNA expression of Nestin, Math1, ChAT, Neurog, HB9, and GFAP after miR-31 transfection of NSCs. (a) Expression of miR-31 according to the agomir/antagomir treatments. (b) Western blot was used to detect the changes in the protein expression of Nestin, ChAT, and GFAP (markers of NSCs, neurons, and glial cells) after the transfection of miR-31. (c) Immunofluorescence was used to detect the differentiation of cells into NSCs after miR-31 transfection. (A color version of this figure is available in the online journal.)

spinal cord, and tail. The loss of the zebrafish tail is a classic phenotype in which the proliferation of zebrafish stem cells is inhibited.[18] Ohnmacht *et al.* [19] showed that in the first 48 h of zebrafish development, its notochord has a strong regenerative ability, which means that at this stage, the zebrafish's central nervous system has a large number of NSCs. In the present study, after miR-31 was knocked down, nervous system development disorders appear and cannot be repaired. Heart abnormalities were also observed in 8 dpf that the blood could not be pumped out, causing pericardial swelling and so on (Supplementary Figure S4), as supported by previous studies that suggested a regulation of heart development by the notochord.[20,21] Therefore, we speculate that the number of NSCs in the zebrafish notochord is severely low after miR-31 knockdown. The apoptotic particles are probably apoptotic NSCs, and there are no sufficient NSCs for normal neural development, and insufficient differentiation leads to developmental disorders of the zebrafish's nervous system. Through the detection of apoptotic particles, we found that the apoptotic particles appeared in the brain and spinal cord, but not in the lateral cord. Therefore, it is speculated that the apoptotic particles are mainly caused by the apoptosis of NSCs, not by its differentiation into MNs.

miR-31 agomir transfection in mouse NSCs and mouse models of SCI elevated the expression of Nestin and decreased ChAT and GFAP (Figures 5 and 6) miR-31 induces the proliferation of mouse NSCs by upregulating the Notch signaling pathway; Notch was inhibited by miR-31 inactivation (Figures 5 and 6) Injection of miR-31 agomir into SCI mouse models could effectively restore motor functions after SCI, which was achieved by promoting the proliferation of endogenous NSCs (Figures 7 and 8) miRNA

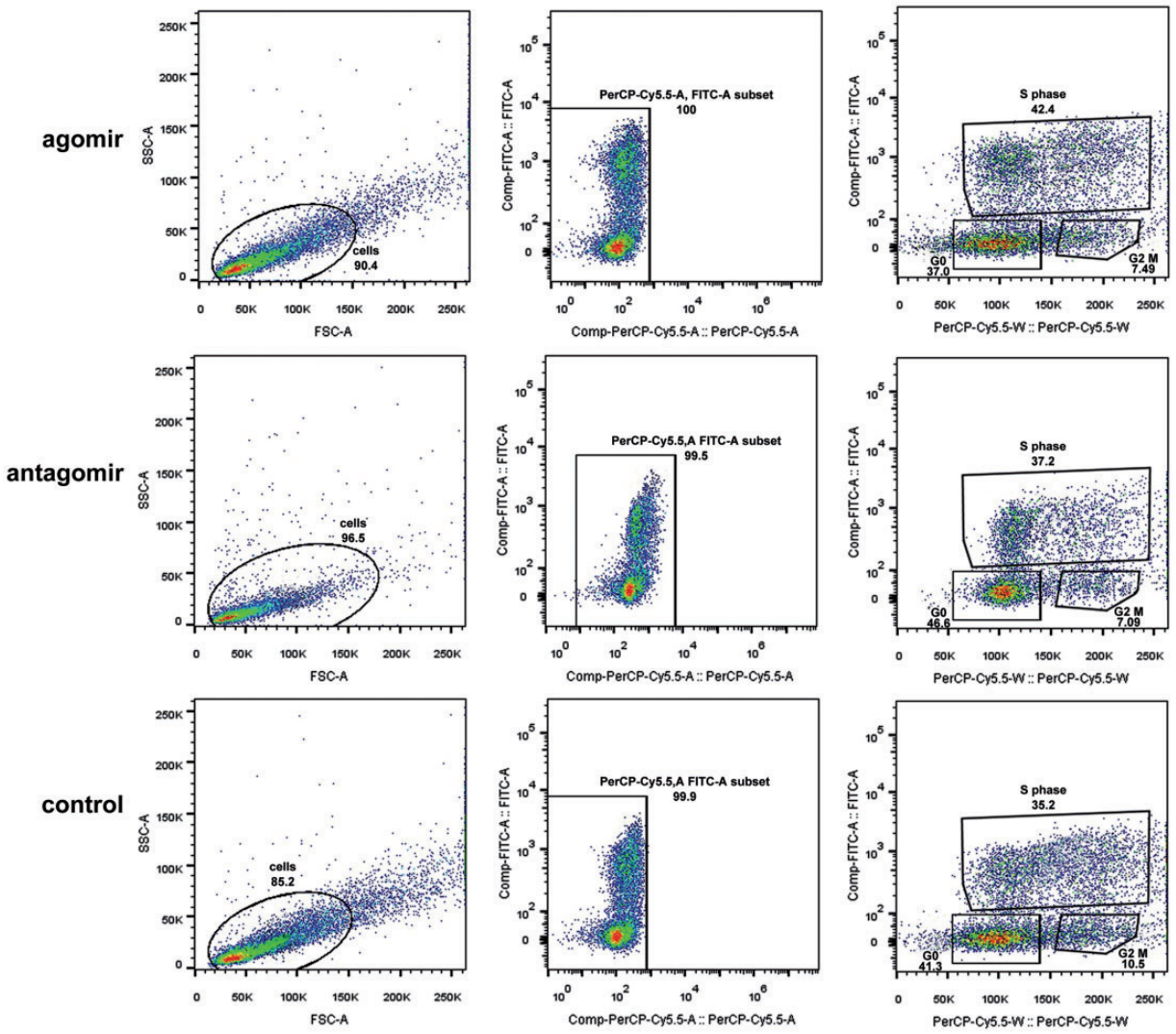

Figure 6. The cell cycle was analyzed by flow cytometry after the transfection of miR-31 into NSCs. Scale bar = 10 μm. *$P < 0.05$. Columns, mean; bars, SEM. (A color version of this figure is available in the online journal.)

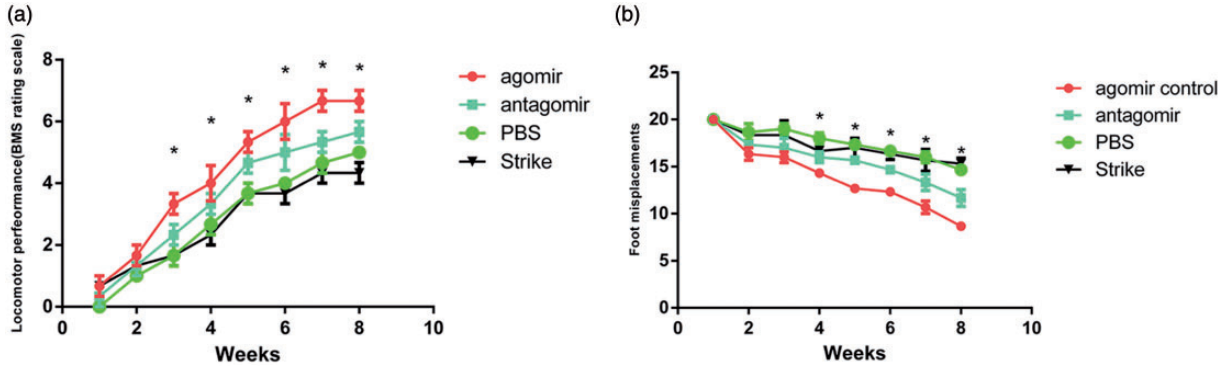

Figure 7. Motor function of mice treated with miR-31 agomir or antagomir. When walking on the open ground, the motor function of the hind limbs of the mice was assessed by BMS ($n = 6$) (a). The mice walked 20 steps on the screen paper, and the number of steps they had missed in their hind limbs was assessed ($n = 6$) (b). The results are shown as means ± SEM. *$P < 0.05$. (A color version of this figure is available in the online journal.)

are involved in proliferation, differentiation, and apoptosis. In early experiments, the miRNA expression profiles were compared between NSCs and neurons, revealing a series of differentially expressed miRNAs, especially mir-31. Furthermore, miR-29, miR-31, and miR-21 are highly expressed in NSCs.[22] Most studies of miR-31 focused on glioblastosarcoma, in which migration and invasion are promoted by miR-31 downregulation,[23,24] and the

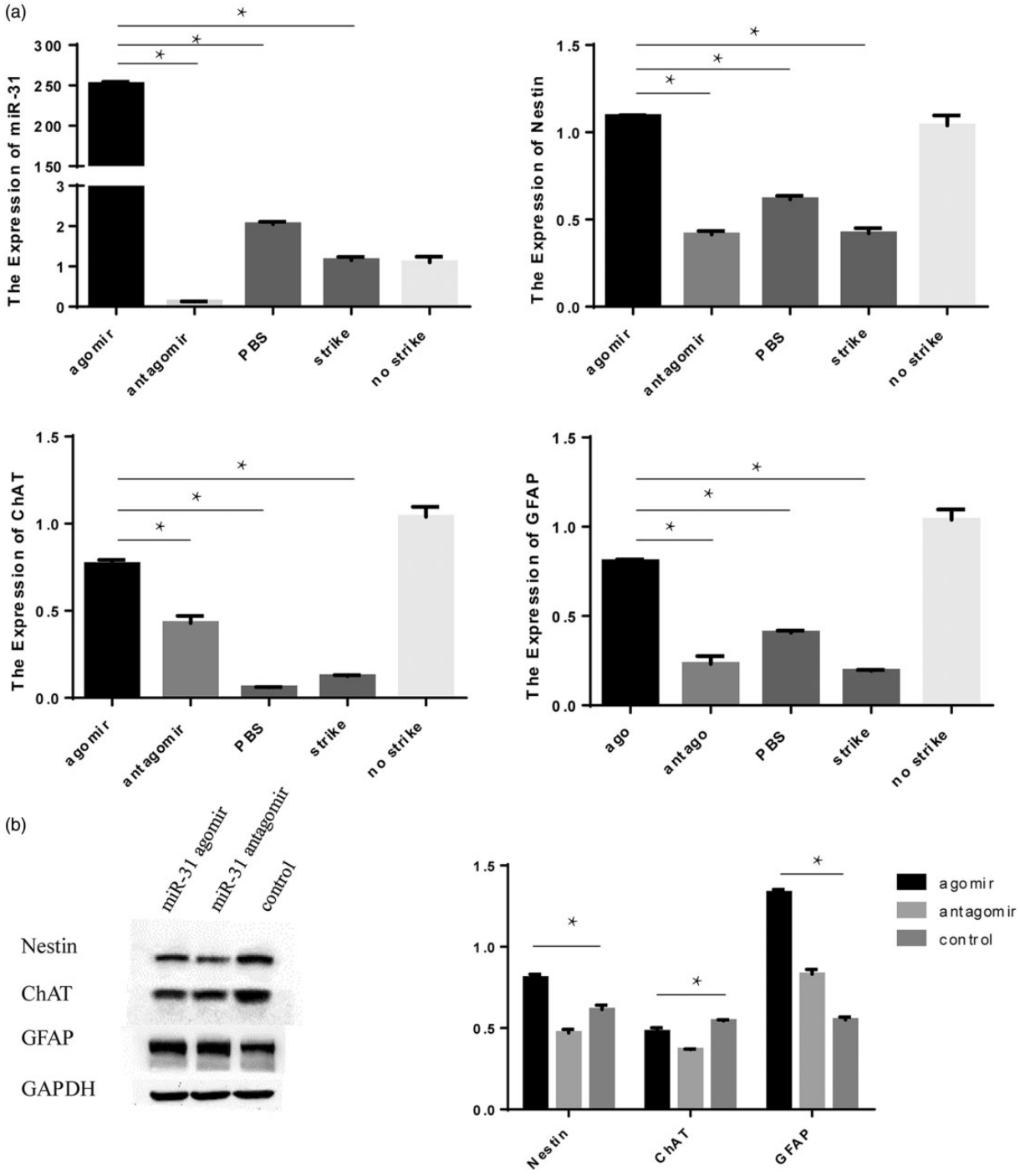

Figure 8. *In vivo* experiments of miR-31. The expression of miR-31, Nestin, ChAT and GFAP at the SCI site was observed after miR-31 injection (a). The protein expression of Nestin, ChAT, and GFAP analyzed by Western blot (b).

up-regulation of miR-31 has tumor inhibition function.[8,23,25,26] Nevertheless, this cannot explain the high mir-31 expression in NSCs and the upregulated expression after SCI.

The Notch signaling pathway is crucially involved in nervous system development [27,28] and in neural development.[29–34] In particular, Donoviel *et al.* [35] found that fetal mice with presenilins gene knockout would have abnormal neural tube development, which was similar to the neural system damage observed in zebrafish. They indicated that the Notch signaling pathway is related to the nervous system. Nervous system development is blocked when Notch signaling is inhibited, which is related to the lateral inhibition mechanism of the Notch signaling pathway.[26,29,30,36,37] In particular, Zilian *et al.* [31] confirmed that Numb gene homozygous inactivation might cause neural tube malformation in fetal rats, and Numb was identified to be the miR-31 target.[32] We speculate that miR-31 is highly expressed in NSCs, inhibits the expression of Numb, and promotes Notch signaling activation, thereby affecting the nervous system.

The sequence of miR-31 is highly conserved among species, and zebrafish was therefore selected to observe the effect of miR-31 on the nervous system (Table 2). Zebrafish models can be applied to the study of the development, gene and drug screening, phenotypic analysis,[33,34,38] and neurological diseases.[19,39,40] In the present study, the motor functions of 48-hpf zebrafish were lost after miR-31 MO. By immunofluorescence, a large number of motor neurons were found to be missing. The results indicate that when miR-31 is knocked out, zebrafish have a high probability of nervous system development obstruction and motor neuron loss, and miR-31 plays a central role in nervous system development.

We cultured NSCs *in vitro* and transfected them with miR-31 agomir or antagomir. No significant reduction was seen in the antagomir group. The decrease in the Agomir group could be because miR-31 attenuated the proliferation of NSCs. The over-expression of miR-31 can upregulate the neural stem cell marker Nestin.[41] Accordingly, immunofluorescence showed that the number of NSCs in the agomir group was higher than in the other groups. Cell cycle analysis showed that miR-31 might prompt NSC proliferation and inhibit NSC differentiation into neurons and glial cells. The antagomir group showed that inhibition of miR-31 expression could promote the differentiation of NSCs and reduce the number of NSCs. Therefore, we believe that miR-31 overexpression can promote the maintenance of the stemness phenotype, while inhibition plays an opposite role in promoting NSC differentiation. Nevertheless, the assessment of the Notch signaling pathway shows that with the overexpression of miR-31, the Numb expression is inhibited, and the Notch signaling pathway is activated. Downstream HES1 and Mash1 are upregulated, indicating that miR-31 regulates the proliferation and differentiation of NSCs after the activation of the Notch signaling *in vitro.*

Currently, researchers have designed agomir to be used *in vivo*, which can be effectively used in many tissues, including the CNS.[42] In this experiment, spinal cord miR-31 was upregulated after injection of the miR-31 agomir. The miR-31 antagomir decreased the miR-31 expression, suggesting that miR-31 agomir and antagomir can be successfully used *in vivo*. Some researchers have confirmed that intravenous miR-124 injection can prevent persistent pain in rats [43] and that intravenous miR-21 antagomir injection caused overexpression of pro-apoptotic genes, increased cell death, and decreased recovery of hind limb motor function.[44] Combined with previous experiments, we speculate that the local injection of miR-31 agomir after SCI could promote SCI repair. The motor function score confirmed that miR-31 agomir injection had a recovery effect after SCI. RT-PCR and Western blotting showed higher Nestin expression in the agomir group compared with the other groups. This indicated that miR-31 agomir injection at the initial stage of injury promoted the proliferation of NSCs and enhanced the recovery effect.

There are some other effects of miR-31 that might be relevant for the treatment of SCI. Studies showed that microglia are involved in the formation of protective scarring during SCI repair, which protects neurons after SCI.[45,46] On the other hand, the high expression of miR-31 will negatively regulate IL-34 expression,[47] which may inhibit the proliferation of microglia and reduce the neuroprotection of microglia after SCI. In addition, decreased vitamin D is detrimental to the repair of SCI,[48,49] which was confirmed by Zhang *et al.*, who showed that vitamin D could upregulate IL-34 in SH-SY5Y neural cells.[50] Therefore, the timely intake of vitamin D during the treatment of SCI may slow down the inhibitory effect of miR-31 on IL-34, which is beneficial to repair after SCI. Nevertheless, vitamin D was not examined in the present study, and future studies will have to investigate vitamin D on the drug delivery mode of miR-31 in the treatment of SCI.

In conclusion, the zebrafish experiments prove that a lack of miR-31 will block nervous system development. In mouse models of SCI, the overexpression of miR-31 might promote SCI repair, involving the Notch signaling pathway.

Table 2. Mature sequence of miR-31is conserved in species.

Species	Sequence 5′ 3′
Human	*aggcaagaugcuggcauagcu*
Rattus	*aggcaagaugcuggcauagcug*
Mouse	*aggcaagaugcuggcauagcug*
Chicken	*aggcaagauguuggcauagcug*
Zebrafish	*ggcaagauguuggcauagcug*

AUTHORS' CONTRIBUTIONS

XL and CW designed experiments. XL, YG, FT, FL, PL, and YY performed the experiments. RD analyzed data. XL and CW wrote the paper. All the authors read the approved the manuscript.

DECLARATION OF CONFLICTING INTERESTS

The author(s) declared no potential conflicts of interest with respect to the research, authorship, and/or publication of this article.

FUNDING

The author(s) disclosed receipt of the following financial support for the research, authorship, and/or publication of this article: This work was supported by the National Natural Science Foundation of China (Grant No. 81371384) and Key Research and Development Projects of Shanxi Province (Grant No. 201803D31068).

DATA AVAILABILITY

The datasets used and/or analyzed during the current study are available from the corresponding author on reasonable request.

ORCID iD

Chunfang Wang https://orcid.org/0000-0002-4138-9097

REFERENCES

1. Salewski RP, Mitchell RA, Shen C, Fehlings MG. Transplantation of neural stem cells clonally derived from embryonic stem cells promotes recovery after murine spinal cord injury. *Stem Cells Dev* 2015;**24**:36–50
2. Grégoire CA, Goldenstein BL, Floriddia EM, Barnabé-Heider F, Fernandes KJ. Endogenous neural stem cell responses to stroke and spinal cord injury. *Glia* 2015;**63**:1469–82
3. Wei H, Wang C, Zhang C, Li P, Wang F, Zhang Z. Comparative profiling of microRNA expression between neural stem cells and motor neurons in embryonic spinal cord in rat. *Int J Dev Neurosci* 2010;**28**:545–51
4. Houbaviy HB, Murray MF, Sharp PA. Embryonic stem cell-specific MicroRNAs. *Dev Cell* 2003;**5**:351–8
5. Liu NK, Wang XF, Lu QB, Xu XM. Altered microRNA expression following traumatic spinal cord injury. *Exp Neurol* 2009;**219**:424–9
6. Xu Y, Zhang X, Pu S, Wu J, Lv Y, Du D. Circulating microRNA expression profile: a novel potential predictor for chronic nervous lesions. *Acta Biochim Biophys Sin* 2014;**46**:942–9
7. Chang HL, Wang HC, Chunag YT, Chou CW, Lin IL, Lai CS, Chang LL, Cheng KI. miRNA expression change in dorsal root ganglia after peripheral nerve injury. *J Mol Neurosci* 2017;**61**:169–77
8. Bleeker FE, Molenaar RJ, Sieger L. Recent advances in the molecular understanding of glioblastoma. *J Neurooncol* 2012;**108**:11–27
9. Liu X, Cheng Y, Chen X, Yang J, Xu L, Zhang C. MicroRNA-31 regulated by the extracellular regulated kinase is involved in vascular smooth muscle cell growth via large tumor suppressor homolog 2. *J Biol Chem* 2011;**286**:42371–80
10. Wang J, Yan CH, Li Y, Xu K, Tian XX, Peng CF, Tao J, Sun MY, Han YL. MicroRNA-31 controls phenotypic modulation of human vascular smooth muscle cells by regulating its target gene cellular repressor of E1A-stimulated genes. *Exp Cell Res* 2013;**319**:1165–75
11. Kimmel CB, Ballard WW, Kimmel SR, Ullmann B, Schilling TF. Stages of embryonic development of the zebrafish. *Dev Dyn* 1995;**203**:253–310
12. Kanungo J, Lantz S, Paule MG. In vivo imaging and quantitative analysis of changes in axon length using transgenic zebrafish embryos. *Neurotoxicol Teratol* 2011;**33**:618–23
13. Rietze RL, Reynolds BA. Neural stem cell isolation and characterization. *Methods Enzymol* 2006;**419**:3–23
14. Hasegawa K, Chang YW, Li H, Berlin Y, Ikeda O, Kane-Goldsmith N, Grumet M. Embryonic radial glia bridge spinal cord lesions and promote functional recovery following spinal cord injury. *Exp Neurol* 2005;**193**:394–410
15. Nasevicius A, Ekker SC. Effective targeted gene 'knockdown' in zebrafish. *Nat Genet* 2000;**26**:216–20
16. Pedrioli DM, Karpanen T, Dabouras V, Jurisic G, van de Hoek G, Shin JW, Marino D, Kalin RE, Leidel S, Cinelli P, Schulte-Merker S, Brandli AW, Detmar M. miR-31 functions as a negative regulator of lymphatic vascular lineage-specific differentiation in vitro and vascular development in vivo. *Mol Cell Biol* 2010;**30**:3620–34
17. Basso DM, Fisher LC, Anderson AJ, Jakeman LB, Mctigue DM, Popovich PG. Basso mouse scale for locomotion detects differences in recovery after spinal cord injury in five common mouse strains. *J Neurotrauma* 2006;**23**:635–59
18. Wang YH, Cheng CC, Lee WJ, Chiou ML, Pai CW, Wen CC, Chen WL, Chen YH. A novel phenotype-based approach for systematically screening antiproliferation metallodrugs. *Chem Biol Interact* 2009;**182**:84–91
19. Ohnmacht J, Yang Y, Maurer GW, Barreiro-Iglesias A, Tsarouchas TM, Wehner D, Sieger D, Becker CG, Becker T. Spinal motor neurons are regenerated after mechanical lesion and genetic ablation in larval zebrafish. *Development* 2016;**143**:1464–74
20. Fouquet B, Weinstein BM, Serluca FC, Fishman MC. Vessel patterning in the embryo of the zebrafish: guidance by notochord. *Dev Biol* 1997;**183**:37–48
21. Goldstein AM, Fishman MC. Notochord regulates cardiac lineage in zebrafish embryos. *Dev Biol* 1998;**201**:247–52
22. Saugstad JA. MicroRNAs as effectors of brain function with roles in ischemia and injury, neuroprotection, and neurodegeneration. *J Cereb Blood Flow Metab* 2010;**30**:1564
23. Hua D, Ding D, Han X, Zhang W, Zhao N, Foltz G, Lan Q, Huang Q, Lin B. Human miR-31 targets radixin and inhibits migration and invasion of glioma cells. *Oncol Rep* 2012;**27**:700–6
24. Zhang B, Li H, Yin C, Sun X, Zheng S, Zhang C, Shi L, Liu Y, Lu S. Dock1 promotes the mesenchymal transition of glioma and is modulated by MiR-31. *Neuropathol Appl Neurobiol* 2017;**43**:419–32
25. Zhou RJ, Xu XY, Liu BX, Dai WZ, Cai MQ, Bai CF, Zhang XF, Wang LM, Lin L, Jia SZ. Growth-inhibitory and chemosensitizing effects of microRNA-31 in human glioblastoma multiforme cells. *Int J Mol Med* 2015;**36**:1159–64
26. Mizutani K, Yoon K, Dang L, Tokunaga A, Gaiano N. Differential notch signalling distinguishes neural stem cells from intermediate progenitors. *Nature* 2007;**449**:351–5
27. Geng X, Sun T, Li JH, Zhao N, Wang Y, Yu HL. Electroacupuncture in the repair of spinal cord injury: inhibiting the notch signaling pathway and promoting neural stem cell proliferation. *Neural Regen Res* 2015;**10**:394–403
28. Zhou QZ, Zhang G, Long HB, Lei F, Ye F, Jia XF, Zhou YL, Kang JP, Feng DX. Effect of spinal cord extracts after spinal cord injury on proliferation of rat embryonic neural stem cells and notch signal pathway in vitro. *Asian Pac J Trop Med* 2014;**7**:562–7
29. Nagao M, Sugimori M, Nakafuku M. Cross talk between notch and growth factor/cytokine signaling pathways in neural stem cells. *Mol Cell Biol* 2007;**27**:3982–94
30. Shimojo H, Ohtsuka T, Kageyama R. Oscillations in notch signaling regulate maintenance of neural progenitors. *Neuron* 2008;**58**:52–64
31. Zilian O, Saner C, Hagedorn L, Lee HY, Säuberli E, Suter U, Sommer L, Aguet M. Multiple roles of mouse numb in tuning developmental cell fates. *Curr Biol* 2001;**11**:494–501
32. Wang JY, Zhou TJ, Sun ZW, Ye T. Zeb1 regulates the symmetric division of mouse lewis lung carcinoma stem cells through numb mediated by miR-31. *Int J Biol Sci* 2018;**14**:1399–410 Jul 28
33. Lieschke GJ, Currie PD. Animal models of human disease: zebrafish swim into view. *Nat Rev Genet* 2007;**8**:353–67
34. Zon LI, Peterson RT. In vivo drug discovery in the zebrafish. *Nat Rev Drug Discov* 2005;**4**:35–44
35. Donoviel DB, Hadjantonakis AK, Ikeda M, Zheng H, Hyslop PS, Bernstein A. Mice lacking both presenilin genes exhibit early embryonic patterning defects. *Genes Dev* 1999;**13**:2801–10
36. Hitoshi S, Seaberg RM, Koscik C, Alexson T, Kusunoki S, Kanazawa I, Tsuji S, Van dKD Primitive neural stem cells from the mammalian epiblast differentiate to definitive neural stem cells under the control of notch signaling. *Genes Dev* 2004;**18**:1806–11
37. Hitoshi S, Alexson T, Tropepe V, Donoviel D, Elia AJ, Nye JS, Conlon RA, Mak TW, Bernstein A, Van dKD. Notch pathway molecules are essential for the maintenance, but not the generation, of mammalian neural stem cells. *Genes Dev* 2002;**16**:846–58
38. Santoriello C, Zon LI. Hooked! Modeling human disease in zebrafish. *J Clin Invest* 2012;**122**:2337–43
39. Boon KL, Xiao S, McWhorter ML, Donn T, Wolf-Saxon E, Bohnsack MT, Moens CB, Beattie CE. Zebrafish survival motor neuron mutants exhibit presynaptic neuromuscular junction defects. *Hum Mol Genet* 2009;**18**:3615–25
40. Peitsaro N, Kaslin J, Anichtchik OV, Panula P. Modulation of the histaminergic system and behaviour by alpha-fluoromethylhistidine in zebrafish. *J Neurochem* 2003;**86**:432–41
41. Lendahl U, Zimmerman LB, Mckay RD. CNS stem cells express a new class of intermediate filament protein. *Cell* 1990;**60**:585–95
42. Krützfeldt J, Rajewsky N, Braich R, Rajeev KG, Tuschl T, Manoharan M, Stoffel M. Silencing of microRNAs in vivo with 'antagomirs'. *Nature* 2005;**438**:685–9
43. Willemen HL, Huo XJ, Mao-Ying QL, Zijlstra J, Heijnen CJ, Kavelaars A. MicroRNA-124 as a novel treatment for persistent hyperalgesia. *J Neuroinflammation* 2012;**9**:143

44. Hu JZ, Huang JH, Zeng L, Wang G, Cao M, Lu HB. Anti-apoptotic effect of microRNA-21 after contusion spinal cord injury in rats. *J Neurotrauma* 2013;**30**:1349–60
45. Bellver-Landete V, Bretheau F, Mailhot B, Vallières N, Lessard M. Microglia are an essential component of the neuroprotective scar that forms after spinal cord injury. *Nat Commun* 2019;**10**:518
46. Veremeyko T, Yung AWY, Dukhinova M, Strekalova T. Ponomarev ED. The role of neuronal factors in the epigenetic reprogramming of microglia in the normal and diseased central nervous system. *Front Cell Neurosci* 2019;**13**:453
47. Li M, Dong Y, Chen Z, Meng L, Liu X, Zhang X, Wang H, Mao W, Zhang J, Jiang Z, Huang T, Hu J, Luo P, Korner H, Ying S, Li J. MicroRNA-31 negatively regulates interleukin-34 expression in vitro. *Immunol Invest* 2019;**48**:597–607
48. Barbonetti A, Cavallo F, D'Andrea S, Muselli M, Felzani G, Francavilla S, Francavilla F. Lower vitamin D levels are associated with depression in people with chronic spinal cord injury. *Arch Phys Med Rehabil* 2017;**98**:940–6
49. Barbonetti A, D'Andrea S, Martorella A, Felzani G, Francavilla S, Francavilla F. Low vitamin D levels are independent predictors of 1-year worsening in physical function in people with chronic spinal cord injury: a longitudinal study. *Spinal Cord* 2018;**56**:494–501
50. Zhang D, Li M, Dong Y, Zhang X, Liu X, Chen Z, Zhu Y, Wang H, Liu X, Zhu J. 1α,25-Dihydroxyvitamin D3 up-regulates IL-34 expression in SH-SY5Y neural cells. *Innate Immun* 2017;**23**:584–91

(Received August 26, 2020, Accepted February 1, 2021)